4-2020

Correcting tree-ring δ13C time series for tree-size effects in eight temperate tree species

Matthew A. Vadeboncoeur
University of New Hampshire, Durham, matt.vad@unh.edu

Katie A. Jennings
University of New Hampshire, Durham

Andrew P. Ouimette
University of New Hampshire, Durham

Heidi Asbjornsen
University of New Hampshire, Durham

Recommended Citation

Vadeboncoeur MA, Jennings KA, Ouimette AP, Asbjornsen H. 2020. Correcting tree-ring δ13C time series for tree-size effects in eight temperate tree species. Tree Physiology, 40(3): 333-349. doi:10.1093/treephys/tpz138

Correcting tree-ring $\delta^{13}C$ time series for tree-size effects in eight temperate tree species

Matthew A. Vadeboncoeur [1] *

Katie A. Jennings [1]

Andrew P. Ouimette [1]

Heidi Asbjornsen [1,2]

1. Earth Systems Research Center, University of New Hampshire, 8 College Road, Durham, NH USA

2. Department of Natural Resources and the Environment, University of New Hampshire, 56 College Road, Durham, NH USA

* corresponding author: matt.vad@unh.edu +1-603-862-4448

Key words:
water-use efficiency, carbon isotopes, ecophysiology, carbon fertilization, subcanopy gradients

Abstract

Stable carbon isotope ratios ($\delta^{13}C$) in tree rings have been widely used to study changes in intrinsic water-use efficiency (iWUE), sometimes with limited consideration of how C-isotope discrimination is affected by tree height and canopy position. Our goals were to quantify the relationships between tree size or tree microenvironment and wood $\delta^{13}C$ for eight functionally diverse temperate tree species in northern New England, and to better understand the physical and physiological mechanisms underlying these differences. We collected short increment cores in closed-canopy stands and analyzed $\delta^{13}C$ in the most recent 5 years of growth. We also sampled saplings in both shaded and sun-exposed environments. In closed-canopy stands, we found strong tree-size effects on $\delta^{13}C$, with 3.7 – 7.2‰ of difference explained by linear regression vs. height (0.11 – 0.28‰ m^{-1}), which in some cases is substantially stronger than the effect reported in previous studies. However, open-grown saplings were often isotopically more similar to large codominant trees than to shade-grown saplings, indicating that light exposure contributes more to the physiological and isotopic differences between small and large trees than does height. We found that in closed-canopy forests, $\delta^{13}C$ correlations with DBH were nonlinear but also strong, allowing a straightforward procedure to correct tree- or stand-scale $\delta^{13}C$-based iWUE chronologies for changing tree size. We demonstrate how to use such data to correct and interpret multi-decadal composite isotope chronologies in both shade-regenerated and open-grown tree cohorts, and we highlight the importance of understanding site history when interpreting $\delta^{13}C$ time series.

Introduction

Stable carbon isotope ratios ($\delta^{13}C$; Coplen 2011) in tree rings (or any plant tissue; $\delta^{13}C_p$) have been widely used to estimate intrinsic water use efficiency (iWUE), defined as the ratio of photosynthesis to stomatal conductance (McCarroll and Loader 2004). These measurements are potentially of great importance for physiologists interested in how the fundamental balance between transpiration and photosynthesis may be shifting due to a variety of global change factors, ranging from changes in climate (Lévesque et al. 2014, Zhang et al. 2018) to acid deposition (Thomas et al. 2013). Such measurements can also be helpful in identifying water stress in managed forests (Fischer and du Toit 2019). However, the driver of changing iWUE that has received the most attention (Franks et al. 2013, Babst et al. 2014, Schubert and Jahren 2015, Frank et al. 2015) has been the dramatic increase in the atmospheric concentration of CO_2 (c_a) from 280 ppm to > 400 ppm since the mid-18th Century (Keeling et al. 1989, 2017), due to theoretical expectations of a strong but likely nonlinear effect of c_a on water-use efficiency (McCarroll et al. 2009, Frank et al. 2015, Voelker et al. 2016). Large and sustained increases in water-use efficiency would likely have important consequences for primary production, ecosystem water balance, and surface energy balances, all of which represent large potential feedbacks to the global climate system (Bonan 2008).

Tree-ring studies of iWUE have sometimes been undertaken without correcting for the potential isotopic effects of tree growth, though often a tree's earliest years of growth are excluded from analysis, due to well-documented "juvenile effects". This term refers to factors which depress iWUE in young trees relative to canopy trees due to differences between canopy and sub-canopy conditions, as well as increasing hydraulic resistance with height. This isotopic juvenile period has been found to last from <15 years in *Quercus* (Raffalli-Delerce et al. 2004) to perhaps centuries in temperate rainforest conifers (Stuiver et al. 1984), but for most species estimates range from 20 – 50 years (Loader et al. 2007, Gagen et al. 2008, Leavitt 2010). If the net effect of changing tree size and canopy position on $\delta^{13}C_p$ are substantial and not accounted for, it would complicate the ability to infer changes in iWUE at the stand

scale from isotopic time-series of individual trees. Failure to account for such effects could also lead to a misattribution of age-driven iWUE trends to drivers such as CO_2 or climate.

There are several distinct mechanisms by which the iWUE of trees can vary with height and canopy position, generally leading to more ^{13}C-depleted signatures in understory trees relative to the canopy trees on the same site. These mechanisms include reduced light below the canopy, which reduces rates of photosynthesis relative to the top of the canopy, increasing CO_2 concentrations inside the leaf (c_i) and therefore reducing discrimination against the assimilation of ^{13}C (Francey and Farquhar 1982). Meanwhile, greater humidity and lower radiational heating in the sub-canopy limit the rate of transpiration and the need for understory trees to down-regulate stomatal conductance. These effects interact with the lower photosynthetic capacity of shade leaves relative to sun-exposed leaves (Boardman 1977, Ellsworth and Reich 1993) and the greater thickness and lower mesophyll conductance of sun leaves, which should reduce the effective average c_i (Schleser and Jayasekera 1985).

The sub-canopy environment can also introduce isotopic effects not related to water-use efficiency, including those driven by below-canopy gradients of c_a and the stable C isotope signature of atmospheric CO_2 ($\delta^{13}C_a$) due to the mixing of the free atmosphere with CO_2 produced by soil respiration (Schleser and Jayasekera 1985, Buchmann et al. 2002). Using free-atmosphere values of $\delta^{13}C_a$ and c_a (as opposed to site-specific below-canopy values, which are rarely measured) may therefore bias calculations of iWUE in understory trees. Another effect which can bias the calculation of iWUE from $\delta^{13}C_p$ is the re-fixation of ^{13}C-depleted respired CO_2 in photosynthetic bark tissues, which should also disproportionately affect young trees with thin bark (Cernusak et al. 2001).

Independent of effects mediated by the sub-canopy microenvironment, changes in height can also have a direct effect on iWUE, due to the increased effect of gravity and hydraulic path resistance on xylem water potential with height (Koch et al. 2004, Coble and Cavaleri 2015). It has even been proposed that hydraulic limitation is a key mechanism limiting tree height and NPP as trees grow, though

the importance of this limitation likely varies widely across species and climates (Ryan and Yoder 1997, Ryan et al. 2006). In contrast, in species where rooting depth continues to increase as trees grow upward through the canopy, larger trees may have access to more reliable water than do juvenile understory trees (Dawson 1996, Ivanov et al. 2012, Brum et al. 2019), which could mitigate or even reverse the effect of tree size on iWUE under dry conditions.

Of the effects discussed above, only the direct effect of height and the increase in rooting depth with growth necessarily change over the lifetimes of the first cohort of trees to colonize an open environment, such as abandoned agricultural land, clearcuts, or burned forests. In contrast, in terms of light, humidity, c_a, and $\delta^{13}C_a$, this early-successional cohort effectively spends its entire life in dominant or codominant positions under full sunlight and exposed to the free atmosphere, reducing the possible position-driven changes in iWUE and $\delta^{13}C_p$ with growth. Trees in stands with more open canopy structure, including savannas and woodlands, or stands thinned by land managers, likely also see less dramatic changes in canopy position-driven iWUE over their lifetimes than trees that regenerate in the shade of a dense canopy.

In contrast to strictly "juvenile" effects that are typically thought to be isolated to a tree's earliest few decades of development, Brienen et al. (2017) showed that in 3 deciduous angiosperm species, the effect of tree size on iWUE is fairly linear throughout much of a tree's life (or at least over a century), and corresponds more directly with height and DBH than with age. This makes simple juvenile-period rules-of thumb suspect, at least when applied outside systems where such effects have been quantified. If these findings apply widely, some reported observations of changes in iWUE in both modern and paleo tree-ring records (e.g. see reviews by Peñuelas et al. 2011, Franks et al. 2013, Voelker et al. 2016) may be overstated or misinterpreted.

In order to design effective global-change studies and accurately interpret tree-ring $\delta^{13}C_p$ time series, researchers require information about the various physical and physiological mechanisms by which iWUE

and $\delta^{13}C_p$ change as a tree grows. A concerted effort is necessary to determine whether published data about the effect of tree size on $\delta^{13}C_p$ are representative of various taxonomic and functional groups of forest trees, as well as different forest stand structures. This study is aimed at better understanding these processes in closed-canopy forests in a humid temperate climate. Our specific questions were:

1. How does the $\delta^{13}C$ of tree-ring α-cellulose vary with height, canopy position, and DBH, across eight functionally diverse temperate tree species sampled in multiple stands?
2. To what extent do the mechanisms discussed above each contribute to changes in both iWUE and $\delta^{13}C_p$ as trees grow?
3. Does removing the isotopic effect of tree growth change the interpretation of multi-decadal composite isotope chronologies?

Methods

Study design

While many dendro-isotopic studies focus primarily on the largest and oldest trees (e.g. Giguère-Croteau et al. 2019), this approach is not always feasible or advisable when the goal is to characterize changes in regions heavily dominated by secondary forests, such as the northeastern United States. Understanding the role of tree physiological responses in long-term hydrological change (e.g. Vadeboncoeur et al. 2018), requires representative and scalable estimates of growth and iWUE.

So-called "juvenile effects" in tree-ring isotopes have typically been detected and quantified by comparing complete tree-ring $\delta^{13}C_p$ time series from trees of different ages (Loader et al. 2007, Gagen et al. 2008), though a few studies have examined recent tree-ring $\delta^{13}C_p$ among co-occurring trees of different sizes in which height, DBH, and canopy position are directly measured (e.g. Leavitt 2010, Brienen et al. 2017). To effectively isolate the effects of tree size and micro-environment on tree physiology from responses to changing climate, c_a, and other global change factors such as acid deposition, our study takes this latter space-for-time approach, and is ultimately aimed at understanding

how to size-correct tree-ring iWUE chronologies from closed-canopy, secondary forests in the northeastern United States.

Sampling for $\delta^{13}C_p$

Tree core samples were collected in 2017-18 from eight common northeastern U.S. tree species which have at least intermediate shade tolerance (Burns and Honkala 1990) and can be found in closed-canopy understories (in approximate order of increasing shade tolerance and dominance in late-successional forests): *Fraxinus americana* L., *Pinus strobus* L., *Quercus rubra* L., *Acer rubrum* L., *Acer saccharum* Marshall, *Picea rubens* Sarg., *Fagus grandifoila* Ehrh., and *Tsuga canadensis* (L.) Carrière. Each species was sampled in two to four stands in New Hampshire and Vermont. Additional sampling effort was allocated to *Picea rubens* and *Acer saccharum*, which have received particular attention regarding to their sensitivity to climate change and acid deposition (Hamburg and Cogbill 1988, Lane et al. 1993, Vadeboncoeur et al. 2012, Bishop et al. 2015, Mathias and Thomas 2018, Kosiba et al. 2018).

Sampled stands (Table S1) were all secondary forests that regenerated naturally after agricultural abandonment, timber harvest, or fire. All were closed-canopy, mixed-species stands with no record or evidence of stand-scale disturbance in the past 30 years. Across these sites, mean annual temperature ranges from 4 – 9ºC, and mean annual precipitation ranges from 1160 – 1340 mm. To reduce variation in iWUE unrelated to tree size, we took care to sample in flat or mid-slope positions, avoiding high-moisture microsites near streams or in depressions, as well as drier microsites with especially rocky or shallow soil.

Our sampling methods were adapted from those of Brienen et al. (2017). Across the full range of tree sizes in each stand, we sampled trees of representative canopy position, health, and vigor for their size. Trees with evidence of a substantial change in canopy position in the previous five years (i.e. loss or dieback of the leader or a major limb on the target tree or a neighboring tree) were not sampled. Samples were sometimes collected within and adjacent to small natural canopy gaps, but we avoided sampling near forest edges and large gaps. Wood samples were collected with a 4.3 mm-diameter increment borer,

to a depth of at most 5 cm into the sapwood (the smallest trees were sampled as shallowly as 5 mm). One sample was collected per tree. Core samples were taken at approximately 30 cm height to minimize the effects of sampling on the timber value of larger trees and the hydraulic function of smaller trees; we do not expect the height of sampling on the bole to systematically affect wood $\delta^{13}C_p$ (Leavitt 2010). Height, diameter at breast height (DBH), and canopy position (using the crown illumination classes of Clark and Clark 1992) were recorded for each sampled tree. The height of each sampled tree was measured from at least two vantage points using a Haglöf Vertex IV hypsometer.

Where available, saplings (defined here as any tree < 4 cm DBH but at least 5 years old) were also included in the analysis, by collecting 5-year old twig segments from the upper, middle, and lower third of the crown. Twig segments were aged by counting terminal bud scars back from a live distal bud. Bark was removed before drying, and lengths proportional to the total 2013 growth of each twig segment were composited for processing.

For most species, additional twig samples were taken opportunistically from saplings growing near one or more of our study stands, on similar soils but in fully illuminated conditions (in recent clearcuts, utility rights-of-way, and clearings around meteorological stations). These samples are intended to help separate the direct effect of absolute size (i.e. hydraulic resistance as affected by height) from those of relative canopy position, and to better represent the initial growth conditions of trees that regenerated following canopy-removing disturbance rather than in the shade of an intact closed canopy. A small number of young saplings were also sampled in a recent strip-cut partial harvest at the Jones site, to provide data on saplings in an intermediate light environment with no canopy directly overhead, but with nearby trees > 20 m tall providing shade for much of the day regardless.

After air-drying samples, growth rings from 2013-17 were identified, measured on a sliding-stage micrometer, and separated from the bark and older wood for isotopic analysis. We analyzed whole rings for all species, due to the difficulty of precisely dividing rings into earlywood and latewood in slowly-growing understory trees. Samples were extracted to α-cellulose using a Jayme-Wise procedure adapted

from Leavitt and Danzer (1993) by Gregg and Brooks (2003). Homogenized samples were analyzed for $\delta^{13}C$ on an Isoprime IRMS at the University of New Hampshire Instrumentation Center. Median $\delta^{13}C$ precision of 15 samples analyzed in duplicate was 0.03‰ (maximum 0.23‰), which reflects both the analytic precision of the mass spectrometer and the degree of sample homogenization.

Calculation of ^{13}C discrimination and iWUE

Tree-ring $\delta^{13}C_p$ measurements can be used to estimate intrinsic water use efficiency (iWUE), defined as the ratio of photosynthesis to stomatal conductance, and calculated as:

$$\mathrm{iWUE} = \frac{c_a\left(b+\delta^{13}C_p-\delta^{13}C_a\right)}{1.6(b-a)} \quad [1]$$

where $\delta^{13}C_a$ is the C isotope ratio of the atmosphere, $\delta^{13}C_p$ is the measured isotope ratio of the plant tissue, *a* is diffusive fractionation against $^{13}CO_2$ = 4.4‰, *b* is fractionation against carboxylation of $^{13}CO_2$ by RuBisCO = 27‰, and 1.6 is the ratio of diffusion rates of water vapor to CO_2 (Farquhar et al. 1982, McCarroll and Loader 2004). An alternative metric (Farquhar et al. 1982), which does not explicitly consider c_a, is ^{13}C discrimination (Δ) relative to the atmosphere:

$$\Delta \equiv \frac{\delta^{13}C_a-\delta^{13}C_p}{1+\frac{\delta^{13}C_p}{1000}} \quad [2]$$

which relates linearly to the ratio of concentrations of intracellular CO_2 (c_i) in the leaf to atmospheric CO_2 (c_a) (Farquhar et al. 1989):

$$\Delta = a + (b - a)\left(\frac{c_i}{c_a}\right) \quad [3]$$

We calculated Δ and iWUE (without attempting to account for post-photosynthetic C fractionation) for each sample using Eqs. 1-2, and assuming that c_a = 401 ppm and $\delta^{13}C_a$= -8.44‰, the mean values observed at Mauna Loa during in 2015 (Keeling et al. 2017, Scripps CO_2 Program 2019). Data on height,

DBH, canopy position, $\delta^{13}C_p$, Δ, and iWUE for all samples have been archived at https://doi.org/10.6073/pasta/de0c8b529b7c2b986eb36d0287397065.

Quanitfying tree size – $\delta^{13}C_p$ relationships

We fit linear regression models to describe the relationship between $\delta^{13}C_p$ and height. Separate models were fitted for trees sampled in closed canopy stands, vs. all trees with crown illumination scores of 4 or 5 including open-grown saplings. For each species, the ratio of the slope of the open regeneration height model to that of the shade regeneration height model was used as a metric of the importance of the various effects of canopy position (light, VPD, c_a, $\delta^{13}C_a$) vs. the direct effect of height on $\delta^{13}C_p$.

Because crown illumination indices are ordinal data, we analyzed the effect of relative canopy position using a Kendall test, expressing the strength of the correlation using Kendall's τ statistic and the magnitude of the effect using the Sen slope.

Our model-fitting procedure for DBH emphasizes the mechanistic differences between codominant and shaded understory and mid-canopy trees, as well as the need to produce a continuous model that can easily be applied to the calculated DBH of each sampled tree at each year of the isotope record. First, we fit a linear regression describing $\delta^{13}C_p$ as a function of DBH, using only the dominant and co-dominant trees (crown classes 4-5) from closed-canopy stands. Where the slope of this regression was non-significant and negative, we instead modeled this relationship with a slope of zero, because overall relationships with size, when they exist, tend to be positive (Figs 1-2; McDowell et al. 2011, Brienen et al. 2017). Next, we fit a similar regression using only the sub-canopy trees (crown classes 1-3). Regression slopes for the sub-canopy trees were always significant and positive. These models intersected at a DBH in the range of the smaller co-dominant trees we sampled. Together, these two models form a segmented linear model describing the expected $\delta^{13}C_p$ of all trees in a closed-canopy forest, or alternatively the expected $\delta^{13}C_p$ of a tree as it grows from the understory into the canopy, hereafter the "closed-canopy model".

Finally, we calculated a line joining the mean DBH and mean $\delta^{13}C_p$ of the open-grown saplings with the breakpoint of the closed-canopy model, to create an "open regeneration" model. Combining this line with the co-dominant segment of the closed-canopy model describes the expected $\delta^{13}C_p$ of a tree as it grows after regenerating in the open.

Correcting composite chronologies for changing tree size

We used three recently collected and previously unpublished composite $\delta^{13}C_p$ chronologies to demonstrate a simple procedure for applying isotopic corrections to remove the effect of tree growth (and therefore create a corrected record in which variation is presumably driven by the effects of climate or other abiotic factors). Sample collection and generation of the example chronologies (*Pinus strobus* and *Quercus rubra/ Q. velutina* at Thompson Farm, plus *Picea rubens* at Cone Pond) are described in supplemental methods. Our correction procedure makes use of the DBH models described above, because DBH is the tree-size parameter which can be directly reconstructed from ring-width chronologies.

To calculate a weighted isotope correction for each year of the three composite isotope time series, we used ring width (R) as a proxy for the contribution of each tree to each year's composite sample. This approach assumes that variation in latewood density, latewood ratio, and % α-cellulose among trees (within a year) are small relative to variation in total ring width. This fractional mass contribution (*F*) to the composite was estimated as:

$$F_{(tree,year)} = \frac{R_{(tree,year)}}{\sum_{tree=1}^{n} R_{(tree,year)}} \quad [4]$$

This step is not applicable to correcting single-tree chronologies (i.e. *F*=1; skip to Eq. 5).

The isotopic correction (*A*) for each tree-year was calculated using a model (*M*) describing $\delta^{13}C_p$ as a function of DBH in a given species. We calculated the difference between modeled $\delta^{13}C_p$ at the tree's current size and the tree's size in each previous year. This correction effectively adjusts the measured isotope value for each year in the past to the size of the tree at the time of sampling:

$$A_{(tree,year)} = M_{(tree\ DBH\ when\ sampled)} - M_{(DBH(tree,year))} \quad [5]$$

For each year in a composite chronology, the weighted mean of tree correction factors can be calculated as:

$$A_{(composite,year)} = \sum_{tree=1}^{n} (F_{(tree,year)} * A_{(tree,year)}) \quad [6]$$

This correction offset value is then added to each annual value in the raw $\delta^{13}C_p$ composite chronology to arrive at a corrected $\delta^{13}C_p$ composite chronology. In cases where it is unclear which model of $\delta^{13}C_p$ as a function of tree size is most appropriate for the history of the sampled trees, multiple models can be applied to illustrate upper and lower constraints for corrected Δ or iWUE.

Vertical gradients in c_a and $\delta^{13}C_a$

To better understand the role that below-canopy vertical gradients in c_a and $\delta^{13}C_a$ play in the observed differences between large and small trees within closed-canopy forest stands, we took advantage of a network of micrometeorological towers recently installed by NEON (Keller et al. 2008). Though not all sites are yet fully operational, there are several in eastern US forests where substantial data were collected in 2018. Each tower collects data on $\delta^{13}C_a$ and c_a at six heights, including one above the canopy. We used data from June-August 2018 to compare three eastern US forest sites: Bartlett Experimental Forest (Bartlett, NH; BART) and Harvard Forest, (Petersham, MA; HARV), which are closed-canopy, hardwood-dominated, New England forests similar in structure to those studied here, and (for contrast) Ordway-Swisher Biological Station (near Gainesville, FL; OSBS), a restored *Pinus palustrus* savanna with a substantially more open canopy. For each 30-minute time interval we calculated the difference between mean c_a and $\delta^{13}C_a$ at each height with that observed at the top of the tower. Because many of these time series showed clear diurnal patterns, we calculated the mean from 10:00 to 15:00 EDT to represent the vertical profile during periods when the canopy is most photosynthetically active. At HARV and OSBS, where $\delta^{13}C_a$ observations were usually asynchronous across the height profile, we estimated $\delta^{13}C_a$ at the top of the tower as the mean of the preceding and subsequent time intervals. The

mean absolute difference between pairs of above-tower observations used for this interpolation was 0.20‰ at HARV and 0.36‰ at OSBS.

Results and Discussion

How does $\delta^{13}C$ of tree-ring α-cellulose vary with height, canopy position, and diameter?

Our observations of $\delta^{13}C$ of wood α-cellulose ($\delta^{13}C_p$) from 8 tree species across 9 forest stands in New Hampshire and Vermont ranged from -33.4‰ to -21.9‰, covering most of the range that has been observed globally for C3 plant tissue (Kohn 2010). Within each species, $\delta^{13}C_p$ varied by as little as 4.3‰ in *Pinus strobus* to as much as 9.8‰ in *Fagus grandifolia*. The variability is largely explained by tree size (expressed either as height or DBH) and by canopy position (Figs 1-3, Tables 1-3), which correlates strongly with size in closed-canopy stands.

Variation with height

Among trees in closed-canopy stands, the relationship between height and $\delta^{13}C_p$ was fairly linear for all species (Fig. 1), with regression slopes ranging from 0.11‰ m^{-1} in *Pinus strobus* to as much as 0.28‰ m^{-1} in *Acer rubrum*. (Fig. 1, Table 1). On average, the slope of these regressions was 0.21‰ m^{-1}. Height regressions explained 3.7 – 7.2‰ of $\delta^{13}C_p$ difference across the height range examined for each species (Fig 1, Table 1).

These closed-canopy tree-height effects on $\delta^{13}C_p$ are large compared with those reported from previous studies. Wood $\delta^{13}C_p$ data reviewed by McDowell et al. (2011) showed height effects averaging 0.07‰ m^{-1} for angiosperms and 0.03‰ m^{-1} for conifers, though reviewed foliar $\delta^{13}C_p$ relationships with height varied more widely. These regression lines are also plotted in Figure 1 for comparison with each of our height regressions; they are sometimes similar in slope to our open-regeneration lines but are always shallower than our shade-regeneration lines, perhaps in some cases reflecting a lesser degree of shading in the trees sampled previously. Brienen et al. (2017), also sampling shaded understory trees along with codominants, found quite consistent height effects of 0.16 – 0.18‰ m^{-1} in the wood of three

angiosperm species (consistent with the wider range we observed), while *Pinus sylvestris* (a shade-intolerant species) had a height effect of approximately zero. Monserud and Marshall (2001), working with three conifer species, report much smaller height effects ranging only up to 0.04‰ m^{-1}, but emphasize that their sampling procedure minimized the influence of shading. The fairly large isotopic effects of tree size that we observed point to a strong combined role of tree size and canopy position on the physiology of all studied species when growing below the forest canopy, and imply that tree size effects should be carefully considered or corrected for when interpreting tree-ring $\delta^{13}C_p$ data, at least in forests similar to those that we studied.

Variation with canopy position

Canopy position as quantified using the crown illumination index also showed strong linear relationships with $\delta^{13}C_p$ (Fig 2, Table 2) across all trees sampled for each species (including the open-grown saplings sampled, which by definition had indices of 4 or 5). This pattern stands in contrast to the fact that open-grown saplings were outliers with regard to the relationship between height and $\delta^{13}C_p$. Sen slopes across numerical indices ranging from 1 to 5 ranged from 0.68‰ (*Pinus strobus*) to 1.75‰ (*Fagus grandifoila*) per crown class, and averaged 1.26‰ (Table 2).

Variation with diameter

In stands with a fairly closed and multi-layered canopy, DBH correlates strongly, if nonlinearly, with both height and the relative position of a tree within the canopy. Among canopy codominant trees, there was only a significant relationship between $\delta^{13}C_p$ and DBH in two species (*Fraxinus americana* and *Tsuga canadensis*; Table 3). These regression slopes averaged 0.02‰ cm^{-1} (after setting negative slopes to zero) and the maximum slope was 0.04‰ cm^{-1} (*F. americana*). In all cases, the slope of the regression for forest subcanopy trees greatly exceeded that of the canopy trees, averaging 0.21‰ cm^{-1} and ranging from 0.08 (*Pinus strobus*) to 0.24 (*Picea rubens*).

The segmented models relating DBH to $\delta^{13}C_p$ (Fig 3, Table 3) emphasize apparent mechanistic differences in the physiological and isotopic consequences of tree growth before vs. after reaching a codominant canopy position. While these models are not to be interpreted as demonstrating a direct mechanistic link between diameter and physiology, they are nevertheless potentially useful. Because DBH is the tree-size parameter which can be directly reconstructed from ring-width chronologies, modeling the relationships between DBH and $\delta^{13}C_p$ provides a straightforward way of correcting for tree growth, at least in species and sites with strong correlations between DBH, height, and light exposure.

The role of species vs. site factors

The apparent greater importance of species than of site in driving the magnitude of isotopic differences between canopy dominants and understory saplings indicates the important role played by species differences in the plasticity and ontogeny of photosynthetic and hydraulic traits (Cavender-Bares and Bazzaz 2000, Rozendaal et al. 2006, Anderegg 2015), as well as differences in C partitioning and transport (Gessler et al. 2014, Bögelein et al. 2019) in mediating the effect of tree growth on $\delta^{13}C_p$ in closed-canopy forests. For example, plasticity in the maximum photosynthetic rate (A_{max}) between shaded and sun-exposed leaves would affect the degree to which c_i and therefore ^{13}C discrimination can be affected by stomatal regulation, while xylem anatomy, rooting depth, and plasticity of hydraulic safety margins and the ratio of sapwood area to leaf area will affect within-tree gradients in water potential and the degree of stomatal closure (Leavitt 2010, McDowell et al. 2011).

Of course, soil characteristics affecting water availability (soil depth, texture, organic content, porosity, and slope position) must also play a role in determining the potential for water stress and therefore stomatal closure, iWUE, and $\delta^{13}C_p$. While most of our sampling avoided extremes of wet or dry soils, this effect is illustrated in our data by two saplings (one *P. rubens* and one *T. canadensis*) sampled at the Cone Pond site, which are plotted as asterisk symbols in Figs 1 and 3, and not included in the regression analyses. These saplings, which were growing in bedrock crevices and surrounded by open

ledge, each plot as less ^{13}C depleted than others of similar size, as would be expected if stomatal conductance is reduced (and iWUE increases) with water limitation.

Because our main questions were about the effects of species and tree size, we sampled across stands with wide range of tree sizes, generally on well-drained soils (Table S2), and in stands with high degree of canopy closure. Across these sites, the pattern of $\delta^{13}C_p$ with tree size and canopy position was quite consistent within a species (Figs 1-3), implying that generating site-specific correction curves for isotopic time-series derived from tree rings might not always be necessary if the species is well characterized and the stand is similar to those for which such curves have been developed.

How do various mechanisms contribute to changes in iWUE and $\delta^{13}C_p$ as trees grow?

A variety of physiological and physical mechanisms have been proposed to explain observed differences in $\delta^{13}C_p$ across trees of different size classes and canopy positions (Table 4). Most of these effects are a consequence of gradients within the canopy, though importantly the direct effect of tree height via hydraulic resistance should operate independent of canopy position. Our data from open-grown saplings can therefore constrain the importance of this direct height effect relative to the others, while data from NEON towers allows us to quantify relevant sub-canopy carbon gradients.

The direct effect of tree size vs canopy position on $\delta^{13}C_p$

The open-grown saplings we sampled tended to be isotopically more similar to large canopy codominant trees of the same species than to understory saplings (Fig. 4a). These open-grown saplings, when compared with similarly-sized trees growing under closed-canopy conditions, as well as with large codominant forest trees, allowed an assessment of the relative importance of a tree's relative canopy position vs. its absolute height in influencing $\delta^{13}C_p$. In contrast to closed-canopy regression slopes averaging 0.21‰ m^{-1}, slopes for regressions including only sun-exposed trees and saplings were much smaller and often not significantly different from zero, ranging from a slightly (though non-significantly) negative slope in *Acer saccharum* to 0.08‰ m^{-1} in *Picea rubens*, and averaging 0.04‰ m^{-1} (Table 1).

We expressed the importance of this direct effect of increasing hydraulic resistance and gravitational loss of water potential with height as the ratio of the slope of the height regression for open-regenerating trees (in which presumably only the direct effect of height is operating) to that of trees regenerating under a closed canopy (in which the effect of height is combined with those of the sub-canopy microenvironment). This ratio ranged from 0% in *Acer saccharum* to 40% in *Picea rubens* (Table 1, Fig. 4b). The highest two ratios we observed (in *Picea rubens* and *Pinus strobus*) were both in conifers, despite the substantial functional and isotopic (Figs 1–3) differences between the two species. This may indicate that, relative to canopy position, the direct effect of size is of greater proportional importance in conifers than in angiosperm tree species. It is also worth noting that conifers are heavily represented in literature on the hydraulic limitation hypothesis (Ryan et al. 2006) and on $\delta^{13}C_p$ variation with tree height (McDowell et al. 2011).

The importance of light (as well as other below-canopy gradients) as a determinant of $\delta^{13}C_p$ has long been recognized (Francey and Farquhar 1982, Ehleringer et al. 1986, Berry et al. 1997, Brooks et al. 1997) with the effect attributed to the strong light limitation of photosynthetic rates (even relative to shade leaves' lower maximum photosynthetic rates), which keeps c_i from ever reaching values as low as it does under light-saturated conditions at the top of the canopy. Our data bear this out, with strong correlations seen between the crown illumination index and $\delta^{13}C_p$ for all eight sample species (Fig 2; these correlations include open-grown saplings which could meaningfully be assigned a crown illumination score). The data from saplings collected from the partial harvest (i.e. living under a partially opened canopy; gray x symbols in Figs 1, 3) also support the important role of canopy position, as they are isotopically intermediate between saplings of similar size growing in either full sun or under a closed canopy. We interpret isotopic differences beyond those directly attributable to height as being primarily driven by high c_i in shaded understory and mid-canopy trees, relative to fully sun-exposed trees (Table 4).

The contribution of below-canopy carbon gradients

At the two northeastern, closed-canopy forest sites within the NEON network, we found a vertical gradient of increasingly depleted ambient $\delta^{13}C_a$ and elevated CO_2 concentrations from above the canopy to near ground level (Fig. 5), likely due to incomplete mixing of the atmosphere down to the ground surface, where soil respiration represents a substantial source (Gaudinski et al. 2000, Ouimette et al. 2018) of ^{13}C-depleted CO_2. The NEON data show that these effects can be substantial within 5 meters of the ground in closed-canopy forests (BART and HARV). Also noteworthy is that the vertical gradients at these two sites were larger than in the temperate forest data reviewed by Brienen et al. (2017), though generally consistent with those observed by Lai et al. (2005), also in northeastern forests. Moreover, careful examination of Figs 1 and 3 shows that the smallest trees we sampled (smaller than about 5 cm DBH or 5 m height), frequently fall well below the regression line (i.e. are 1 – 2‰ more depleted than would be expected from the trend observed in intermediate trees), consistent with depletion in $\delta^{13}C_a$ observed at these heights (Fig 5a). However, growth-years represented by these small saplings, which were included in our analysis for the sake of completeness in assessing mechanisms, would normally be excluded from isotopic analysis using juvenile-period rules-of-thumb. We observed little if any isotopic difference from the free atmosphere above 5 m in the closed-canopy stands. In the more open stand at OSBS, we observed little systematic difference from the free atmosphere at any height.

The effect of vertical gradients in c_a on $\delta^{13}C_p$ depends in part on the physiology and hydraulic strategy of the trees that are predominantly photosynthesizing at heights below 5 m. One might expect that in densely shaded understory conditions, where photosynthesis rates are slow and evaporative demand is low, there is little potential for a C fertilization effect on iWUE. However, we can illustrate the degree to which isotopic estimates of c_i/c_a and iWUE are affected by using a free-atmosphere c_a value in place of a more realistic sub-canopy c_a value. For example, at a height of 2.8 m, mid-day c_a averages 42 ppm above free-atmosphere values at the Bartlett tower. This approximately 10% excess in c_a would translate to underestimation of iWUE by approximately 10% if the free-atmosphere c_a is used in place of the actual

ambient c_a (Eqs 1–3). Based on the patterns seen in Fig 5, this 10% value represents an approximate upper bound for this effect, again for trees of a size that are rarely included in isotopic chronologies.

Does removing the isotopic effect of tree growth change the interpretation of multi-decadal composite isotope chronologies?

The data collected for this study allowed us to generate segmented regression models relating $\delta^{13}C_p$ to DBH for a given species, and under open or shaded regeneration conditions (Fig. 3; Table 3), which can be used to remove the effect of tree growth from tree-ring $\delta^{13}C$ time series prior to the calculation of iWUE chronologies which can then be related to climatic and atmospheric data.

To demonstrate the application of $\delta^{13}C_p$ corrections to composite isotope chronologies, we selected three previously unpublished chronologies (methods supplement; Table S3) encompassing a variety of functional groups as well as varying stand histories. Due to species differences in the DBH-$\delta^{13}C_p$ models, as well as known differences in the initial growth conditions within each study stand, the corrections we applied to the three example chronologies varied substantially in magnitude (Fig. 6; note that positive corrections to $\delta^{13}C_p$ translate to negative corrections to Δ of almost equal magnitude, see Eq. 2). For example, at 1950, the $\delta^{13}C_p$ correction for shade-regenerated *Picea rubens* at Cone Pond, was +1.16‰, while for open-grown *Pinus strobus* at Thompson Farm, the correction was only +0.42‰ (+10.0 and +3.6 μmol/mol respectively in terms of iWUE; Fig S1). Moreover, the *P. strobus* correction is quite small throughout most of the chronology, only exceeding 0.1‰ before 1962, and does not alter the conclusion that this time series has no long-term trend in Δ (Fig. 6b). For *P. rubens*, the correction reduces the magnitude of the apparent decline in Δ (i.e. increase in iWUE) prior to about 1990, but does not affect the reversal of this trend (similar to that seen by Mathias and Thomas (2018) in more southern *P. rubens*) after that date (Fig 6a). In contrast, for *P. strobus*, the correction has no appreciable effect on the interpretation of changing Δ or iWUE (Figs 6, S1).

At Thompson Farm, the *P. strobus* cohort is older than the *Quercus* cohort (Table S3), and *P. strobus* tree rings show a release in the 1950s, while most of the *Quercus* sampled seem to have germinated shortly after this event. Interpreting this as a stand-thinning partial harvest, we therefore show both the open-grown correction as well as the closed canopy correction for *Q. rubra* in Fig 6, recognizing that the true needed correction is intermediate between these two options. The mean of these two corrections (partial-open correction in Fig 6), is consistent with saplings sampled in the thinned stand at the Jones site (Fig 3g). For 1976, the earliest year of this chronology, the closed-canopy correction is +2.15‰ (due to the small average size of the sampled trees at this date; Table S3), while the open-regeneration correction is only +0.31‰. In this case, the partial-open correction changes the interpretation of this 40-year chronology from approximately stable Δ and increasing iWUE (including any growth effects on iWUE), to increasing Δ and stable iWUE (after removing growth effects). This finding is consistent with that found by Marshall and Monserud (1996) in western conifers (i.e. apparent changes in iWUE were not present after correcting for height).

There are a variety of other model-fitting procedures that could be reasonably applied to describe the non-linear relationship between DBH, depending on the assumptions made and the variable of interest. For illustrative purposes, we chose a method which is easily interpreted, and which lends itself to be applied as a correction based directly on DBH. The magnitude of the required correction is well constrained by the data, however.

Recommendations for applying corrections to chronologies

When applying tree-size corrections to $\delta^{13}C_p$ chronologies, our data show that it is important to understand the regeneration conditions of the stand. For highly shade-intolerant species, one can assume regeneration in at least partially open conditions, but most long-lived species that are of interest to dendrochronology, especially in closed-canopy mesic forests, have some degree of shade tolerance, as do all of the species studied here. At some sites, stand management and disturbance history might be documented or easily reconstructed from aerial photographs. In other cases, the ring-width chronologies

themselves offer important clues, including the establishment dates of various cohorts, growth rates through the sapling stage, and the timing of release events (Pederson et al. 2014). This is illustrated by the Thompson Farm stand which followed a common post-agricultural successional and management trajectory seen across much of the northeast (Foster et al. 2008, Vadeboncoeur et al. 2012). Using such data appropriately to select a tree-size correction (if any) is critical to correctly interpreting long-term time series of Δ, and particularly when iWUE or c_i/c_a are to be scaled to infer quantitative fluxes of water and carbon between forests and the atmosphere. Correlations of Δ or iWUE with climatic data might also be improved after correcting for tree-size effects, though the value of the "juvenile" (i.e. shaded) life stage in such analyses is debatable (Arneth et al. 2002, Leavitt 2010), and should be carefully considered given the study system and question at hand.

Our data suggest that some species (e.g. *Pinus strobus*) require smaller corrections than other species (e.g. *Fagus grandifolia*), even when the sampled trees originated in a shaded understory. Focusing on species in which successful regeneration predominantly occurs in large gaps or following a stand-resetting disturbance (e.g. *P. strobus, Fraxinus americana*) rather than those that are highly shade-tolerant (e.g. *Tsuga canadensis, F. grandifolia, Acer saccharum, Picea rubens*) may sometimes be an appropriate strategy. In fact, it is worth noting that without management or natural disturbance to the canopy, the understory cohorts of moderately shade-intolerant species such as *P. strobus* and *F. americana* that we sampled are unlikely to survive to maturity.

Brienen et al. (2017) found that tree-size effects on $\delta^{13}C_p$ were smaller in *Pinus sylvestris* than in the angiosperm species they examined, which is fortunate given the importance of this species in global-change studies of Δ (e.g. Gagen et al. 2008). Whether this finding applies to other *Pinus* species remains to be seen, though it is encouraging to consider that *P. strobus* and *P. sylvestris* represent separate subgenera within *Pinus* (see also Monserud and Marshall 2001). However, the speculation by Brienen et al. (2017) that conifers might show less change in Δ with size than angiosperms (see also McDowell et al. 2011) is not supported by our data from *Picea rubens* and *Tsuga canadensis* (Table 1, Fig 1), which are

extremely shade-tolerant and slow-growing relative to most *Pinus* species, and can persist for many decades as saplings under dense, year-round shade.

It is important to emphasize that regardless of whether any correction is applied, the high-frequency variation in $\delta^{13}C_p$ remains meaningful over sufficiently short time periods that canopy position and height can be assumed to be constant. Additionally, corrections for growth may not be needed when studying the effects of experimental manipulations in which treated and control trees are well paired (e.g. Guerrieri et al. 2011, Jennings et al. 2016). In longer-term studies, it would be wise to either correct $\delta^{13}C_p$ for the effect of changing tree size as demonstrated here (Fig. 6), or to verify that the study species, in the context of what is known about stand history, is insensitive to such tree-size effects (e.g. Leavitt 2010; Brienen et al. 2017).

Summary and Conclusions

Across eight temperate tree species representing a variety of life-history and physiological strategies, we found strong relationships between wood $\delta^{13}C$ and tree size and microenvironment, with as much as 7‰ of difference between codominant trees and co-occurring saplings of the same species (Q1). These differences have important consequences for interpreting trends in multidecadal time series of iWUE derived from $\delta^{13}C_p$ in tree rings. Light gradients are likely the dominant factor affecting iWUE and $\delta^{13}C_p$ as trees grow in forests similar to those we studied (Q2). Comparing young saplings growing in open conditions with those under closed canopies showed that the direct effect of height (i.e. via increasing resistance of the hydraulic pathway) accounted for a relatively small fraction of the total variation in $\delta^{13}C_p$, averaging 20%. This hydraulically mediated relationship between height and $\delta^{13}C_p$ was generally in line with height effects reported previously. Sub-canopy gradients in c_a and $\delta^{13}C_a$ only have the potential to substantially bias iWUE estimates in the seedling and early sapling stages, which are easily and routinely excluded from tree-ring $\delta^{13}C$ studies. Species differed substantially in the magnitude of $\delta^{13}C_p$ differences across trees of different sizes, and the mechanisms responsible for this variation deserve

further investigation. The modest effects of site imply that site-specific characterization of this relationship might not always be necessary.

We presented a straightforward methodology that can be used to correct individual trees or multiple-tree composite chronologies in species where DBH is a reasonable (if nonlinear) proxy for height and canopy position. As such, applying $\delta^{13}C_p$ corrections derived from closed-canopy stands would be inappropriate if applied to trees known to have regenerated in full-sunlight conditions. The interpretation of our *Quercus* isotopic chronology changed substantially (from increasing iWUE to stable iWUE) after correcting for changes in tree height and canopy position over 40 years, while correction for tree growth reduced the inferred increases in iWUE in the *Picea rubens* example, and hardly at all in *Pinus strobus* example (Q3). Future studies are needed to expand the diversity of species for which size-$\delta^{13}C$ relationships are quantified, and to better disentangle the various mechanisms driving these relationships.

Data Availability

All original data used to characterize tree-size relationships with $\delta^{13}C_p$ and shown in in Figs 1–4 are available at: https://doi.org/10.6073/pasta/de0c8b529b7c2b986eb36d0287397065

Funding

This work was funded by the National Science Foundation (EAR-1562127 to MV and DEB-1638688 to Scott Olligner), the Iola Hubbard Climate Change Endowment managed by the Earth Systems Research Center at the University of New Hampshire, the New Hampshire Agricultural Experiment Station (Accession #1003450), and the USDA Forest Service Northeastern States Research Cooperative.

Acknowledgements

We thank Cameron McIntire, Stacie Powers, Emily Beard, Taylor Lindsay, Emily Perry, Robert Lafreniere, Kensley Hammond, and Rand Snyder for field and lab assistance. We are grateful to the UNH Office of Woodlands and Natural Areas, the White Mountain National Forest, the USFS Northern Research Station, the US Geological Survey, and the NH Division of Forests and Lands for permission to

collect samples. The comments of three anonymous reviewers helped us to strengthen this work. The National Ecological Observatory Network is a program sponsored by the National Science Foundation and operated under cooperative agreement by Battelle Memorial Institute. This material is based in part upon work supported by the National Science Foundation through the NEON Program. Views expressed in this paper are those of the authors and do not necessarily reflect those of the funding agencies. The use of trade names is for informational purposes only and does not imply endorsement.

References

Anderegg WRL (2015) Spatial and temporal variation in plant hydraulic traits and their relevance for climate change impacts on vegetation. New Phytol 205:1008–1014.

Arneth A, Lloyd J, Šantrůčková H, Bird M, Grigoryev S, Kalaschnikov YN, Gleixner G, Schulze E-D (2002) Response of central Siberian Scots pine to soil water deficit and long-term trends in atmospheric CO_2 concentration. Global Biogeochem Cycles 16:5-1-5–13.

Babst F, Alexander MR, Szejner P, Bouriaud O, Klesse S, Roden J, Ciais P, Poulter B, Frank D, Moore DJP, Trouet V (2014) A tree-ring perspective on the terrestrial carbon cycle. Oecologia:307–322.

Berry SC, Varney GT, Flanagan LB (1997) Leaf $\delta^{13}C$ in *Pinus resinosa* trees and understory plants: Variation associated with light and CO_2 gradients. Oecologia 109:499–506.

Bishop DA, Beier CM, Pederson N, Lawrence GB, Stella JC, Sullivan TJ (2015) Regional growth decline of sugar maple (*Acer saccharum*) and its potential causes. Ecosphere 6:art179.

Boardman NK (1977) Comparative photosynthesis of sun and shade plants. Annu Rev Plant Physiol 28:355–377.

Bögelein R, Lehmann MM, Thomas FM (2019) Differences in carbon isotope leaf-to-phloem fractionation and mixing patterns along a vertical gradient in mature European beech and Douglas fir. New Phytol 222:1803–1815.

Bonan GB (2008) Forests and climate change: forcings, feedbacks, and the climate benefits of forests. Science (80-) 320:1444–9.

Brienen RJW, Gloor E, Clerici S, Newton R, Arppe L, Boom A, Bottrell S, Callaghan M, Heaton T, Helama S, Helle G, Leng MJ, Mielikäinen K, Oinonen M, Timonen M (2017) Tree height strongly affects estimates of water-use efficiency responses to climate and CO_2 using isotopes. Nat Commun 8:288.

Brooks JR, Flanagan LB, Buchmann N, Ehleringer JR (1997) Carbon isotope composition of boreal plants: Functional grouping of life forms. Oecologia 110:301–311.

Brum M, Vadeboncoeur MA, Ivanov V, Asbjornsen H, Saleska S, Alves LF, Penha D, Dias JD, Aragão LEOC, Barros F, Bittencourt P, Pereira L, Oliveira RS (2019) Hydrological niche segregation defines forest structure and drought tolerance strategies in a seasonal Amazon forest Barua D (ed). J Ecol 107:318–333.

Buchmann N, Brooks JR, Ehleringer JR (2002) Predicting daytime carbon isotope ratios of atmospheric CO_2 within forest canopies. Funct Ecol 16:49–57.

Burns RM, Honkala BH (1990) Silvics of North America. USDA Forest Service, Agriculture Handbook 654.

Cavender-Bares J, Bazzaz FA (2000) Changes in drought response strategies with ontogeny in *Quercus rubra*: implications for scaling from seedlings to mature trees. Oecologia 124:8–18.

Cernusak LA, Marshall JD, Comstock JP, Balster NJ (2001) Carbon isotope discrimination in photosynthetic bark. Oecologia 128:24–35.

Clark DA, Clark DB (1992) Life history diversity of canopy and emergent trees in a neotropical rain forest. Ecol Monogr 62:315–344.

Coble AP, Cavaleri MA (2015) Light acclimation optimizes leaf functional traits despite height-related constraints in a canopy shading experiment. Oecologia

Coplen TB (2011) Guidelines and recommended terms for expression of stable-isotope-ratio and gas-ratio measurement results. Rapid Commun Mass Spectrom 25:2538–2560.

Dawson TE (1996) Determining water use by trees and forests from isotopic, energy balance and transpiration analyses: the roles of tree size and hydraulic lift. Tree Physiol 16:263–272.

Ehleringer JR, Field CB, Lin Z, Kuo C (1986) Leaf carbon isotope and mineral composition in subtropical plants along an irradiance cline. Oecologia 70:520–526.

Ellsworth DS, Reich PB (1993) Canopy structure and vertical patterns of photosynthesis and related leaf traits in a deciduous forest. Oecologia 96:169–178.

Farquhar GD, Ehleringer JR, Hubick KT (1989) Carbon Isotope Discrimination and Photosynthesis. Annu Rev Plant Physiol Plant Mol Biol 40:503–537.

Farquhar GD, O'Leary MH, Berry JA (1982) On the relationship between carbon isotope discrimination and the intercellular carbon dioxide concentration in leaves. Aust J Plant Physiol 9:121–137.

Fischer PM, du Toit B (2019) Use of $\delta^{13}C$ as water stress indicator and potential silvicultural decision support tool in *Pinus radiata* stand management in South Africa. iForest - Biogeosciences For 12:51.

Foster DR, Donahue B, Kitteredge D, Motzkin G, Hall B, Turner B, Chilton E (2008) New England's Forest Landscape. Ecological Legacies and Conservation Patterns Shaped by Agrarian History. In: Agrarian Landscapes in Transition. Oxford University Press, New York

Francey RJ, Farquhar GD (1982) An explanation of $^{13}C/^{12}C$ variations in tree rings. Nature 297:28–31.

Frank DC, Poulter B, Saurer M, Esper J, Huntingford C, Helle G, Treydte K, Zimmermann NE, Schleser GH, Ahlström A, Ciais P, Friedlingstein P, Levis S, Lomas M, Sitch S, Viovy N, Andreu-Hayles L, Bednarz Z, Berninger F, Boettger T, D'Alessandro CM, Daux V, Filot M, Grabner M, Gutierrez E, Haupt M, Hilasvuori E, Jungner H, Kalela-Brundin M, Krapiec M, Leuenberger M, Loader NJ, Marah H, Masson-Delmotte V, Pazdur A, Pawelczyk S, Pierre M, Planells O, Pukiene R, Reynolds-Henne CE, Rinne KT, Saracino A, Sonninen E, Stievenard M, Switsur VR, Szczepanek M, Szychowska-Krapiec E, Todaro L, Waterhouse JS, Weigl M (2015) Water-use efficiency and transpiration across European forests during the Anthropocene. Nat Clim Chang 5:579–583.

Franks PJ, Adams MA, Amthor JS, Barbour MM, Berry JA, Ellsworth DS, Farquhar GD, Ghannoum O, Lloyd J, McDowell N, Norby RJ, Tissue DT, von Caemmerer S (2013) Sensitivity of plants to changing atmospheric CO_2 concentration: from the geological past to the next century. New Phytol 197:1077–1094.

Gagen M, McCarroll D, Robertson I, Loader NJ, Jalkanen R (2008) Do tree ring $\delta^{13}C$ series from *Pinus sylvestris* in northern Fennoscandia contain long-term non-climatic trends? Chem Geol 252:42–51.

Gaudinski JB, Trumbore SE, Davidson EA, Zheng S (2000) Soil carbon cycling in a temperate forest: radiocarbon-based estimates of residence times, sequestration rates and partitioning of fluxes. Biogeochemistry 51:33–69.

Gessler A, Ferrio JP, Hommel R, Treydte K, Werner R a, Monson RK (2014) Stable isotopes in tree rings: towards a mechanistic understanding of isotope fractionation and mixing processes from the leaves to the wood. Tree Physiol 34:796–818.

Giguère-Croteau C, Boucher É, Bergeron Y, Girardin MP, Drobyshev I, Silva LCR, Hélie J-F, Garneau M (2019) North America's oldest boreal trees are more efficient water users due to increased [CO_2], but do not grow faster. Proc Natl Acad Sci 116:2749–2754.

Gregg J, Brooks R (2003) Operating procedures for holocellulose and α-cellulose extraction. US EPA Integrated Stable Isotope Research Facility, Corvallis, OR.

Guerrieri R, Mencuccini M, Sheppard LJ, Saurer M, Perks MP, Levy P, Sutton MA, Borghetti M, Grace J (2011) The legacy of enhanced N and S deposition as revealed by the combined analysis of $\delta^{13}C$, $\delta^{18}O$ and $\delta^{15}N$ in tree rings. Glob Chang Biol 17:1946–1962.

Hamburg SP, Cogbill CV (1988) Historical decline of red spruce populations and climatic warming. Nature 331:428–431.

Ivanov VY, Hutyra LR, Wofsy SC, Munger JW, Saleska SR, De Oliveira RC, De Camargo PB (2012) Root niche separation can explain avoidance of seasonal drought stress and vulnerability of overstory trees to extended drought in a mature Amazonian forest. Water Resour Res 48:1–21.

Jennings KA, Guerrieri R, Vadeboncoeur MA, Asbjornsen H (2016) Response of Quercus velutina growth and water use efficiency to climate variability and nitrogen fertilization in a temperate deciduous forest in the northeastern USA. Tree Physiol 36

Keeling CD, Bacastow RB, Carter AF, Piper SC, Whorf TP, Heimann M, Mook WG, Roeloffzen H (1989) A three-dimensional model of atmospheric CO_2 transport based on observed winds: 1. Analysis of observational data. In: Peterson DH (ed) Aspects of Climate Variability in the Pacific and the Western Americas. American Geophysical Union, pp 165–236.

Keeling RF, Graven HD, Welp LR, Resplandy L, Bi J, Piper SC, Sun Y, Bollenbacher A, Meijer HAJ (2017) Atmospheric evidence for a global secular increase in carbon isotopic discrimination of land photosynthesis. Proc Natl Acad Sci:201619240.

Keller M, Schimel DS, Hargrove WW, Hoffman FM (2008) A continental strategy for the National Ecological Observatory Network. Front Ecol Environ

Koch GW, Sillett SC, Jennings GM, Davis SD (2004) The limits to tree height. Nature 428:851–4.

Kohn MJ (2010) Carbon isotope compositions of terrestrial C3 plants as indicators of (paleo)ecology and (paleo)climate. Proc Natl Acad Sci U S A 107:19691–5.

Kosiba AM, Schaberg PG, Rayback SA, Hawley GJ (2018) The surprising recovery of red spruce growth shows links to decreased acid deposition and elevated temperature. Sci Total Environ 637–638:1480–1491.

Lai C-T, Ehleringer JR, Schauer AJ, Tans PP, Hollinger DY, Paw U KT, Munger JW, Wofsy SC (2005) Canopy-scale $\delta^{13}C$ of photosynthetic and respiratory CO_2 fluxes: observations in forest biomes across the United States. Glob Chang Biol 11:633–643.

Lane CJ, Reed DD, Mroz GD, Liechty HO (1993) Width of sugar maple (*Acer saccharum*) tree rings as affected by climate. Can J For Res 23:2370–2375.

Leavitt SW (2010) Tree-ring C-H-O isotope variability and sampling. Sci Total Environ 408:5244–5253.

Leavitt SW, Danzer SR (1993) Method for batch processing small wood samples to holocellulose for stable-carbon isotope analysis. Anal Chem 65:87–89.

Lévesque M, Siegwolf R, Saurer M, Eilmann B, Rigling A (2014) Increased water-use efficiency does not lead to enhanced tree growth under xeric and mesic conditions. New Phytol 203:94–109.

Loader NJ, McCarroll D, Gagen M, Robertson I, Jalkanen R (2007) Extracting climatic information from stable isotopes in tree rings. In: Dawson TE, Siegwolf RTW (eds) Stable Isotopes as Indicators of Ecological Change. Academic Press, pp 46–67.

Marshall JD, Monserud RA (1996) Homeostatic gas-exchange parameters inferred from 13C/12C in tree rings of conifers. Oecologia 105:13–21.

Mathias JM, Thomas RB (2018) Disentangling the effects of acidic air pollution, atmospheric CO 2 , and climate change on recent growth of red spruce trees in the Central Appalachian Mountains. Glob Chang Biol

McCarroll D, Gagen MH, Loader NJ, Robertson I, Anchukaitis KJ, Los S, Young GHF, Jalkanen R, Kirchhefer A, Waterhouse JS (2009) Correction of tree ring stable carbon isotope chronologies for changes in the carbon dioxide content of the atmosphere. Geochim Cosmochim Acta 73:1539–1547.

McCarroll D, Loader NJ (2004) Stable isotopes in tree rings. Quat Sci Rev 23:771–801.

McDowell NG, Bond BJ, Dickman LT, Ryan MG, Whitehead D (2011) Relationships Between Tree Height and Carbon Isotope Discrimination. In: Meinzer FC, Lachenbruch B, Dawson TE (eds) Size- and Age-Related Changes in Tree Structure and Function. Springer, Dordrecht, pp 255–286.

Monserud RA, Marshall JD (2001) Time-series analysis of $\delta^{13}C$ from tree rings. I. Time trends and autocorrelation. Tree Physiol 21:1087–1102.

Ouimette AP, Ollinger SV, Richardson AD, Hollinger DY, Keenan TF, Lepine LC, Vadeboncoeur MA (2018) Carbon fluxes and interannual drivers in a temperate forest ecosystem assessed through comparison of top-down and bottom-up approaches. Agric For Meteorol 256–257

Pederson N, Dyer JM, McEwan RW, Hessl AE, Mock CJ, Orwig DA, Rieder HE, Cook BI (2014) The legacy of episodic climatic events in shaping temperate, broadleaf forests. Ecol Monogr 84:599–620.

Peñuelas J, Canadell JG, Ogaya R (2011) Increased water-use efficiency during the 20th century did not translate into enhanced tree growth. Glob Ecol Biogeogr 20:597–608.

Raffalli-Delerce G, Masson-Delmotte V, Dupouey JL, Stievenard M, Breda N, Moisselin JM (2004) Reconstruction of summer droughts using tree-ring cellulose isotopes: A calibration study with living oaks from Brittany

(western France). Tellus, Ser B Chem Phys Meteorol 56:160–174.

Rozendaal DMA, Hurtado VH, Poorter L (2006) Plasticity in leaf traits of 38 tropical tree species in response to light; relationships with light demand and adult stature. Funct Ecol 20:207–216.

Ryan MG, Phillips N, Bond BJ (2006) The hydraulic limitation hypothesis revisited. Plant, Cell Environ 29:367–381.

Ryan MG, Yoder BJ (1997) Hydraulic limits to tree height and tree growth: What keeps trees from growing beyond a certain height? Bioscience 47:235–242.

Schleser GH, Jayasekera R (1985) $\delta^{13}C$-variations of leaves in forests as an indication of reassimilated CO_2 from the soil. Oecologia 65:536–542.

Schubert BA, Jahren AH (2015) Global increase in plant carbon isotope fractionation following the last glacial maximum caused by increase in atmospheric pCO_2. Geology 43:435–438.

Scripps CO_2 Program (2019) Scripps Institution of Oceanography. http://scrippsco2.ucsd.edu/data/atmospheric_co2/mlo.html

Stuiver M, Burk RL, Quay PD (1984) $^{13}C/^{12}C$ Ratios in Tree Rings and the Transfer of Biospheric Carbon to the Atmosphere. J Geophys Res 89:11,731–11,748.

Thomas RB, Spal SE, Smith KR, Nippert JB (2013) Evidence of recovery of *Juniperus virginiana* trees from sulfur pollution after the Clean Air Act. Proc Natl Acad Sci U S A 110:15319–24.

Vadeboncoeur MA, Green MB, Asbjornsen H, Campbell JL, Adams MB, Boyer EW, Burns DA, Fernandez IJ, Mitchell MJ, Shanley JB (2018) Systematic variation in evapotranspiration trends and drivers across the Northeastern United States. Hydrol Process 32:3547–3560.

Vadeboncoeur MA, Hamburg SP, Cogbill CV, Sugimura WY (2012) A comparison of presettlement and modern forest composition along an elevation gradient in central New Hampshire. Can J For Res 42:190–202.

Voelker SL, Brooks JR, Meinzer FC, Anderson R, Bader MK-F, Battipaglia G, Becklin KM, Beerling D, Bert D, Betancourt JL, Dawson TE, Domec J-C, Guyette RP, Körner C, Leavitt SW, Linder S, Marshall JD, Mildner M, Ogée J, Panyushkina I, Plumpton HJ, Pregitzer KS, Saurer M, Smith AR, Siegwolf RTW, Stambaugh MC, Talhelm AF, Tardif JC, Van de Water PK, Ward JK, Wingate L (2016) A dynamic leaf gas-exchange strategy is conserved in woody plants under changing ambient CO_2: evidence from carbon isotope discrimination in paleo and CO_2 enrichment studies. Glob Chang Biol 22:889–902.

Zhang X, Liu X, Zhang Q, Zeng X, Xu G, Wu G, Wang W (2018) Species-specific tree growth and intrinsic water-use efficiency of Dahurian larch (*Larix gmelinii*) and Mongolian pine (*Pinus sylvestris* var. *mongolica*) growing in a boreal permafrost region of the Greater Hinggan Mountains, Northeaste. Agric For Meteorol 248:145–155.

Table 1. Linear regression statistics relating $\delta^{13}C_p$ to height (ht) for trees sampled in closed-canopy stands. All data and regressions (of the form $\delta^{13}C_p = m\,(\text{ht}) + b$) are graphed in Fig. 1. Height is in meters, and $\delta^{13}C$ is in pemil. nC = number of codominant trees sampled; nO = number of open-grown saplings sampled; nT = total number of trees sampled. Note that we were unable to sample a sufficient number of open-grown *Tsuga canadensis* saplings to generate an open regeneration model.

			Shade regeneration model					***Open regeneration model***							
Species	**min ht**	**max ht**	**nT**	**m**	**m SE**	**b**	**R^2**	**nC**	**nO**	**m**	**m SE**	**b**	**R^2**	**p**	**slope ratio**
ACRU	1.8	25.8	35	0.2814	0.0397	-32.20	0.60	16	2	0.0692	0.0320	-27.16	0.25	**0.048**	0.25
ACSA	1.0	33.7	62	0.1823	0.0178	-31.57	0.64	24	5	-0.0004	0.0209	-26.07	0.00	0.98	0.00
FAGR	0.6	27.8	51	0.2632	0.0236	-33.03	0.72	15	4	0.0189	0.0369	-26.21	0.02	0.62	0.07
FRAM	0.5	32.3	32	0.2214	0.0223	-31.53	0.77	21	4	0.0570	0.0169	-27.06	0.37	**0.003**	0.26
PIRU	0.4	26.1	70	0.2206	0.0191	-28.22	0.66	34	3	0.0892	0.0285	-25.81	0.24	**0.03**	0.40
PIST	0.5	33.6	37	0.1113	0.0160	-28.61	0.58	17	5	0.0371	0.0103	-26.69	0.46	**0.003**	0.33
QURU	1.8	31.9	35	0.1529	0.0215	-31.65	0.60	14	3	0.0186	0.0217	-27.42	0.06	0.41	0.12
TSCA	0.3	26.6	39	0.2072	0.0146	-29.65	0.84								

Table 2. Sen slopes and Kendall τ statistics relating $\delta^{13}C$ to crown illumination classes (Clark and Clark 1992). All data and regressions are graphed in Fig 2. All samples assigned crown illumination score are included.

species	n trees	Sen slope	intercept	Kendall τ
ACRU	37	1.38	-31.76	0.69
ACSA	67	1.40	-32.10	0.67
FAGR	53	1.75	-33.06	0.74
FRAM	36	1.64	-32.91	0.68
PIRU	74	1.02	-28.71	0.56
PIST	42	0.68	-28.78	0.54
QURU	38	1.23	-32.20	0.71
TSCA	41	0.99	-29.30	0.64

Table 3. Segmented linear models relating $\delta^{13}C$ to DBH, for use in correcting $\delta^{13}C$ chronologies for changes in tree size. All data and regressions (of the form $\delta^{13}C = m$ (dbh) + b) are graphed in Fig. 3. DBH is in centimeters, and $\delta^{13}C$ is in pemil. nC = number of codominant trees sampled; nS = number of subcanopy trees sampled; nO = number of open-grown saplings sampled; nT = total number of trees sampled. Intersect DBH indicates the diameter above which the codominant model is to be used; below this diameter, either the open regeneration or forest subcanopy model may be used, depending on the history of the trees to be corrected.

							Forest codominant model					***Forest subcanopy model***					***Open regeneration model***			
Species	**nC**	**nS**	**nO**	**nT**	**min DBH**	**max DBH**	**m**	**m SE**	**b**	**R^2**	**p**	**m**	**m SE**	**b**	**R^2**	**p**	**Intersect DBH**	**m**	**b**	**Notes**
ACRU	14	21	2	**37**	0.6	51.7	0.0186	0.0273	-26.31	-0.04	0.51	0.2142	0.0454	-31.46	0.52	1E-04	26.3	0.0397	-26.86	
ACSA	19	43	5	**67**	0.0	89.1	0	NA	-26.06	NA	NS	0.1293	0.0206	-30.86	0.48	2E-07	37.1	0.0028	-26.16	1
FAGR	13	38	2	**53**	0.0	55.5	0.0420	0.0297	-27.34	0.08	0.18	0.1645	0.0222	-31.82	0.59	9E-09	36.5	0.0075	-26.08	
FRAM	17	15	4	**36**	0.0	72.0	0.0326	0.0083	-26.76	0.47	0.001	0.2007	0.0457	-31.19	0.57	0.001	26.3	0.0358	-26.85	
PIRU	30	40	3	**74**	0.0	54.7	0	NA	-24.09	NA	NS	0.2416	0.0231	-28.86	0.74	9E-13	19.8	0.0956	-25.98	1
PIST	12	25	5	**42**	0.0	62.8	0	NA	-25.72	NA	NS	0.0781	0.0219	-28.47	0.33	0.002	35.2	0.0304	-26.79	1
QURU	11	24	3	**38**	0.6	62.5	0.0321	0.0196	-28.23	0.14	0.14	0.0936	0.0191	-30.83	0.46	4E-05	42.4	0.0130	-27.42	2
TSCA	12	27	2	**41**	0.0	51.8	0.0349	0.0117	-26.43	0.42	0.01	0.1383	0.0186	-29.42	0.68	8E-08				3

Notes:

1: Slope of codominant segment reported as zero rather than as a non-significant negative slope.

2: Initial analysis resulted in no intersection between the two models within the sampled DBH range. Forest subcanopy model was re-run including the smallest three codominant trees to force an interpretable model similar to the other species.

3: Only one suitable open-canopy sapling was sampled, so no open-regeneration model is reported.

Table 4. Summary of mechanisms that may differentially affect $\delta^{13}C_p$ across size classes of co-occurring trees, with conclusions about the importance of each in closed-canopy, temperate forests.

Mechanism	Description of mechanism	Effect on Δ and iWUE	Mediated by stand structure?	Conclusions from this study	Selected references
Direct height (hydraulic) effects	Reduction in leaf water potential due to hydraulic resistance and gravitational effects. The ratio of sapwood area to leaf area may also decline as trees grow. Reduces stomatal conductance, increases iWUE.	Declining Δ (increasing iWUE) as trees grow	No (aside from any allometric plasticity related to stand density)	Sometimes an important factor, driving up to 40% of isotopic differences among trees (Figs 1,4b)	Ryan and Yoder 1997; Monserud and Marshall 2001; Koch et al. 2004; Brienen et al. 2017
Light gradient	Solar radiation increases photosynthetic rates and draw-down of ci. Leaf warming increases transpiration rates, which may lead to stomatal down-regulation, also increasing iWUE. Interacts with leaf plasticity (mesophyll anatomy, Amax) to light conditions.	Declining Δ (increasing iWUE) as trees grow from understory to canopy	Yes	Likely the dominant driver of isotopic differences seen in our sampled trees (Figs 2,4a)	Francey & Farquhar 1982; Schleser & Jayasekera 1985; Brienen et al. 2017
VPD gradient	Humidity is often lower at the top of the canopy than below. Higher VPD may lead to stomatal down-regulation as leaf water potential drops, increasing iWUE.	Declining Δ (increasing iWUE) as trees grow from understory to canopy	Yes	Cannot be separated from the light effect using our data	Von Arx et al. 2013; Davis et al. 2019
Rooting depth	Larger trees may be more deeply rooted in some ecosystems; potentially avoiding water stress and reducing iWUE.	Increasing Δ (declining iWUE) as rooting depth increases	Perhaps, via root competition for water and nutrients?	If present, this effect is overridden by the sum of the others	Dawson 1996; Brum et al. 2018
C re-fixation in bark	Respired (isotopically light) C may be re-fixed by photosynthesis in thin bark that permits light penetration. The importance of this process to whole-tree C balance declines as bark ages.	Spuriously high apparent Δ (spuriously low apparent iWUE) in smaller trees.	No? Dependency may vary with the plasticity and ontogeny of bark anatomy	Cannot be separated from the height effect using our data	Cernusak et al. 2001
Ambient $\delta^{13}C_a$ gradient	Below-canopy CO_2 can be ^{13}C-depleted due to contributions from soil (and plant) respiration.	Using atmospheric $\delta^{13}C_a$ values results in overestimation of understory iWUE	Yes	Small effect, likely only important in the sapling stage (Fig 5a)	Buchmann et al. 2002; Schleser & Jayasekera 1985
Ambient c_a gradient	Greater CO_2 concentrations below canopy due to contribution of soil respiration. Probably does not strongly affect iWUE under low-light conditions.	Using atmospheric ca values results in overestimation of understory iWUE	Yes	Small effect, likely only important in the sapling stage (Fig 5b)	Buchmann et al. 1996

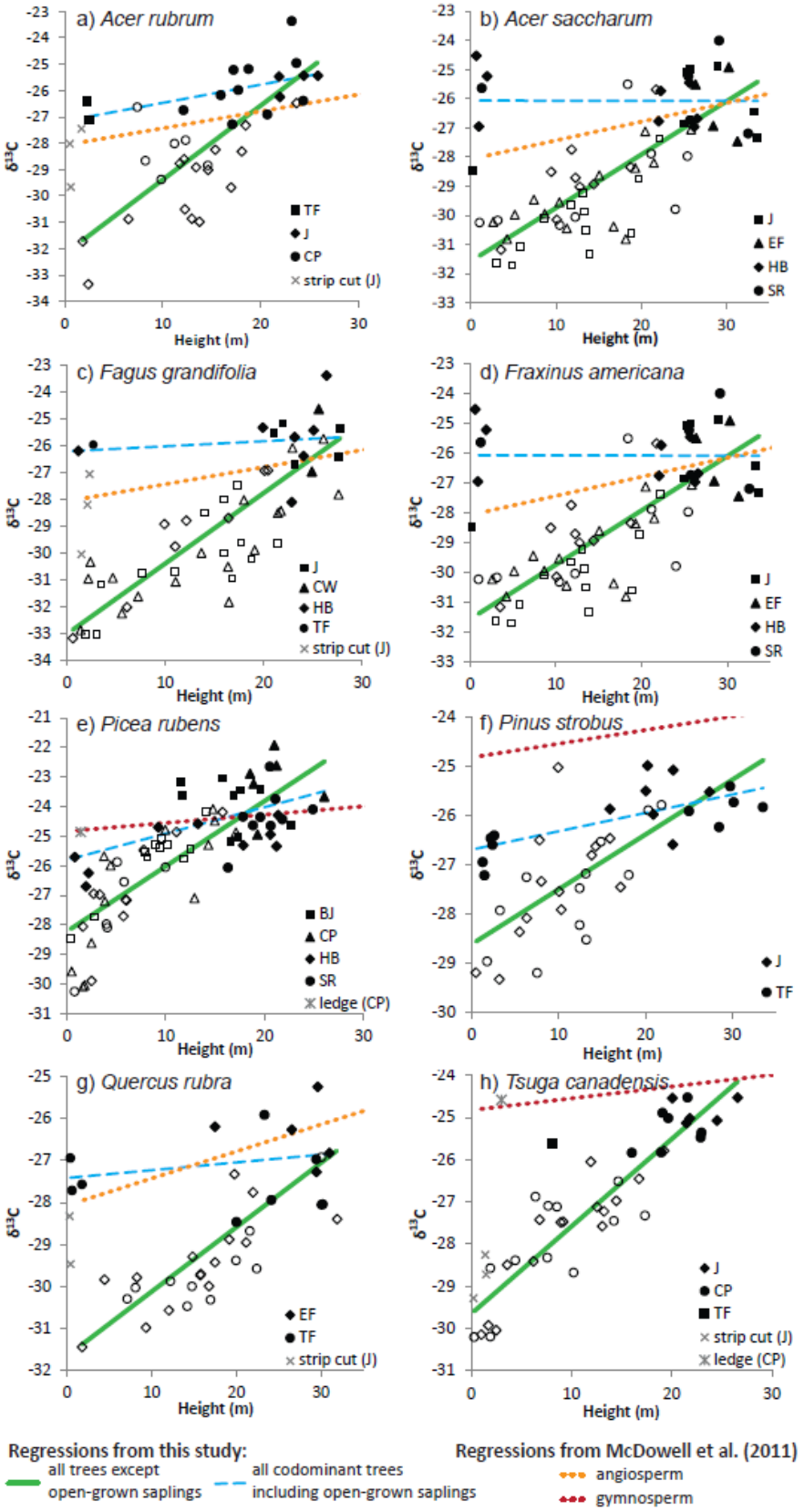

Figure 1: Relationships between height and $\delta^{13}C$ for the eight species sampled. Solid lines show "shade-regeneration" regressions for codominant (filled symbols) and understory trees (open symbols), while broken lines show "open-regeneration" regressions for codominant trees and open-grown saplings.

For comparison, the dotted line shows the regression reported by McDowell et al. (2011) for wood of angiosperm and gymnosperm species, as appropriate. Samples plotted as x and * symbols (saplings from strip-cut partial harvests and open ledge environments, respectively) are included for illustrative purposes only and are not included in the regressions.

Note that x and y axis scales vary by species in order to show all data clearly. Regression statistics are shown in Table 2; site codes are listed in table S1.

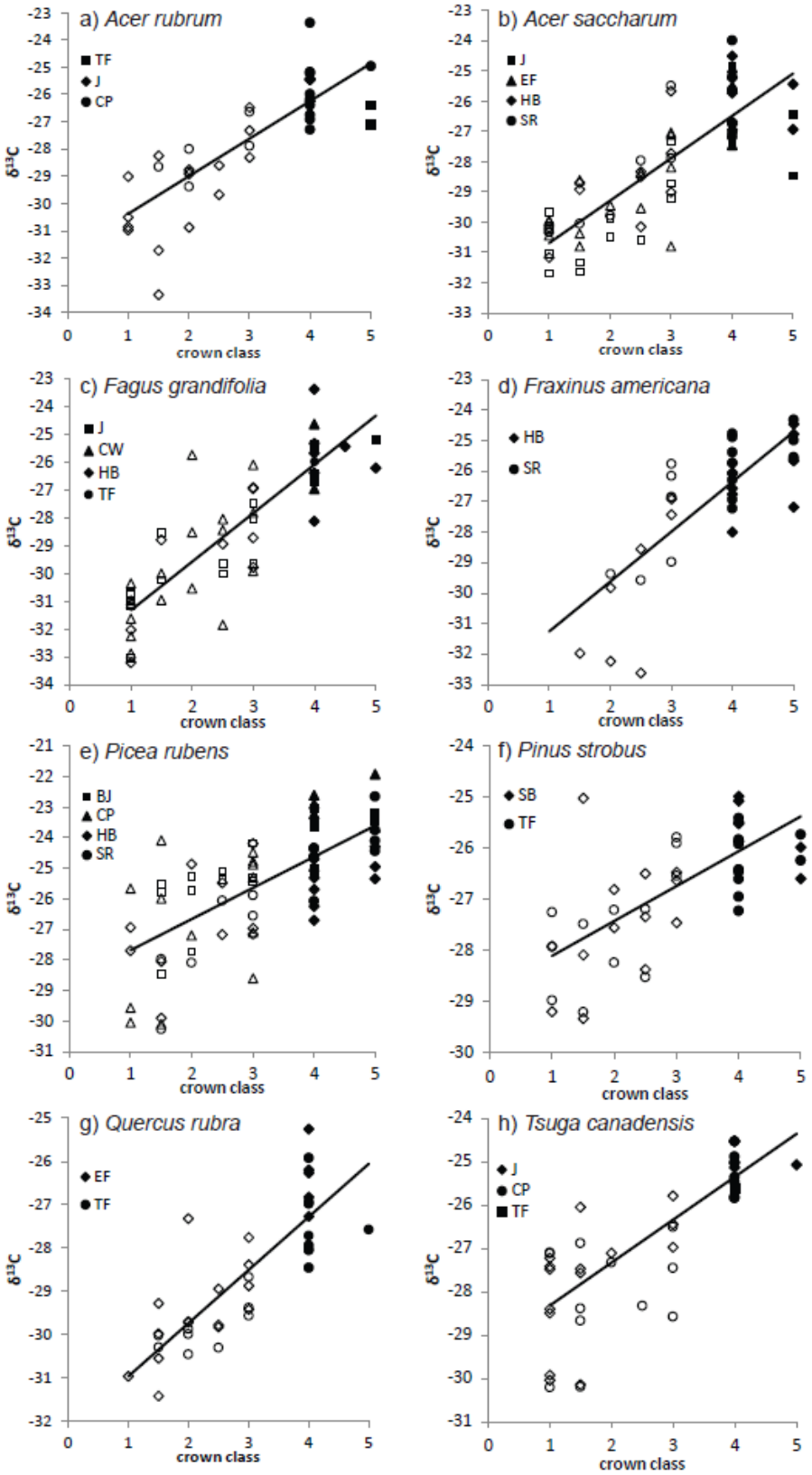

Figure 2: Relationships between crown illumination index (Clark and Clark 1992) and $\delta^{13}C$ for the eight species sampled.

Note that y-axes vary by species. Non-parametric trend statistics are shown in Table 2; site codes are listed in table S1.

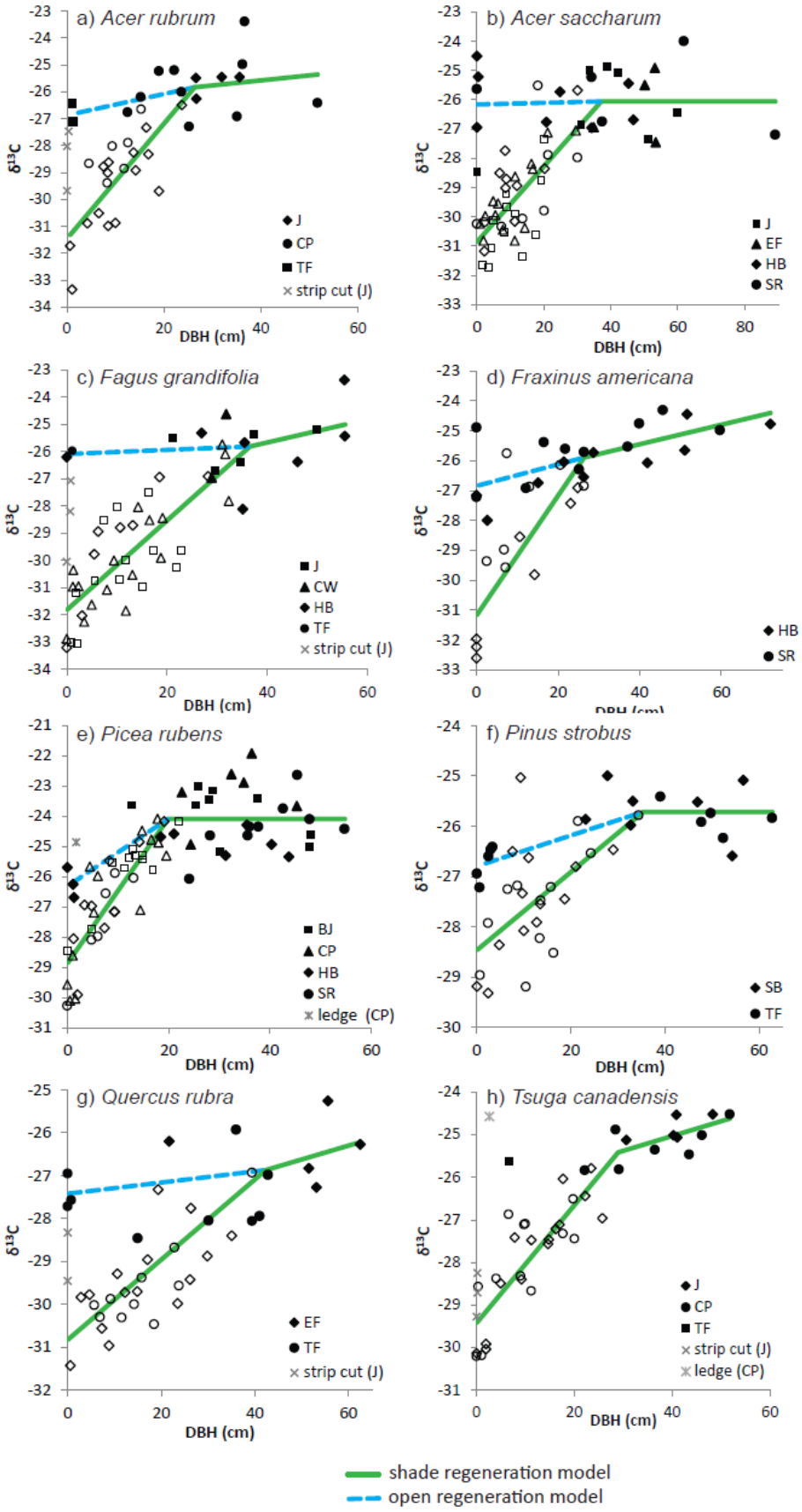

Figure 3: Relationships between DBH and $\delta^{13}C$ for the eight species sampled. Solid lines show models for codominant (filled symbols) and understory trees (open symbols), while broken lines show models for codominant trees and open-grown saplings. Samples plotted as x and * symbols (saplings from strip-cut partial harvests and open ledge environments, respectively) are included for illustrative purposes only and are not included in the regressions.

Note that x and y axis scales vary by species. Regression statistics are shown in Table 1; site codes are listed in table S1.

Figure 4: a) Boxplot comparing δ13C of tree-ring cellulose collected from canopy trees (DBH ≥20 cm and crown score ≥ 4), open-grown saplings (DBH <4 cm and crown score ≥ 4), and understory saplings (DBH <4 cm and crown score < 4).
b) The proportional contribution of the direct effect of height to the total δ13C differences observed across sampled trees, expressed as the ratio of the slope of the open-regeneration height regression to the shade-regeneration height regression. Error bars show ±1 SE. The mean value across these 7 species is 0.20 ± 0.06. No open-grown saplings were sampled for *T. canadensis*, so it is excluded here.

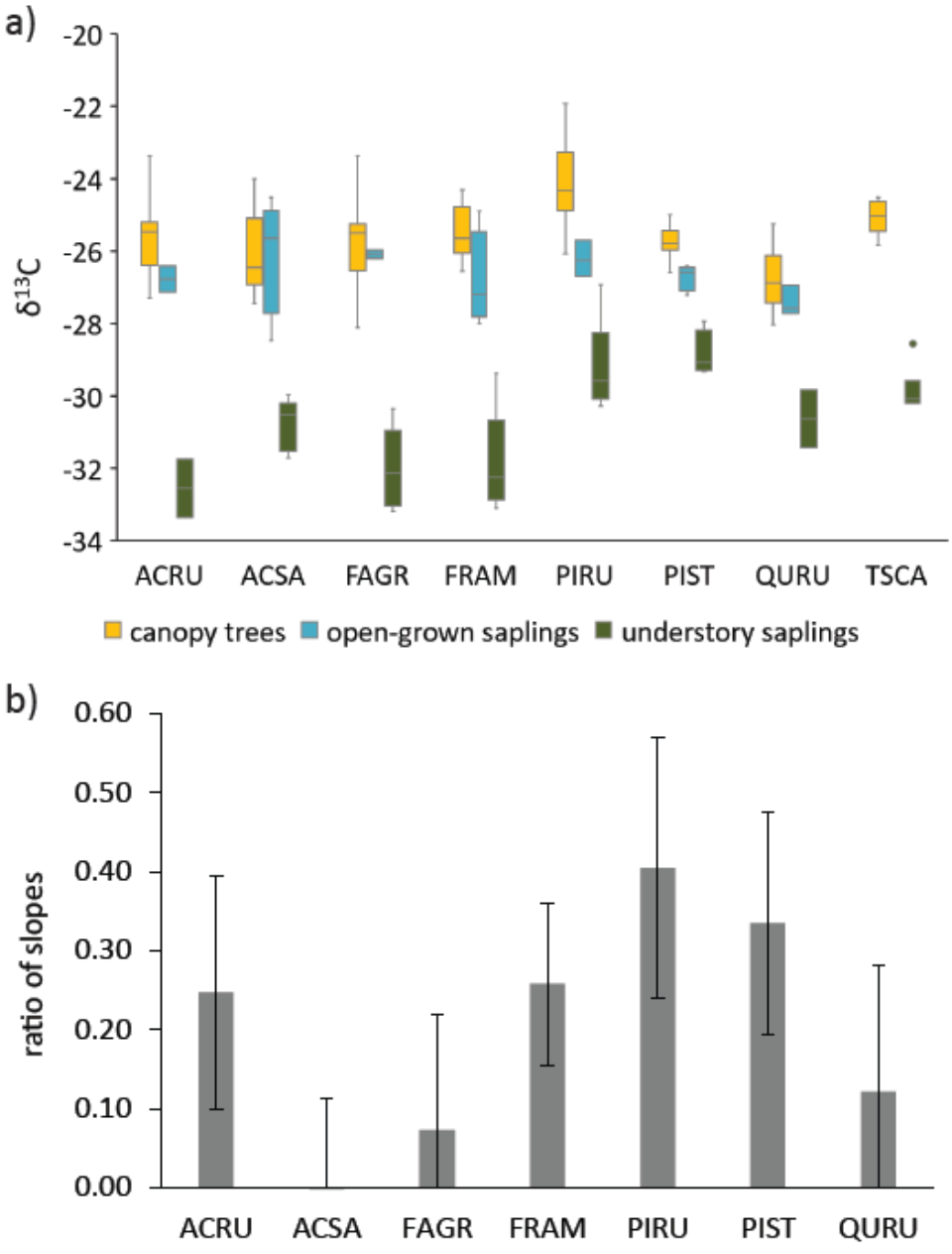

Figure 5: Vertical profiles of ambient c_a and $\delta^{13}C_a$, during peak photosynthetic conditions (10:00-15:00 EDT; June August 2018) at three NEON flux tower sites. Bartlett (BART) and Harvard Forest (HARV) are closed-canopy forests, similar in structure to stands that we sampled. Ordway-Swisher (OSBS), shown for comparison, is a pine savanna with a more open canopy. Canopy height averages 23m at BART and OSBS, and 26m at HARV.

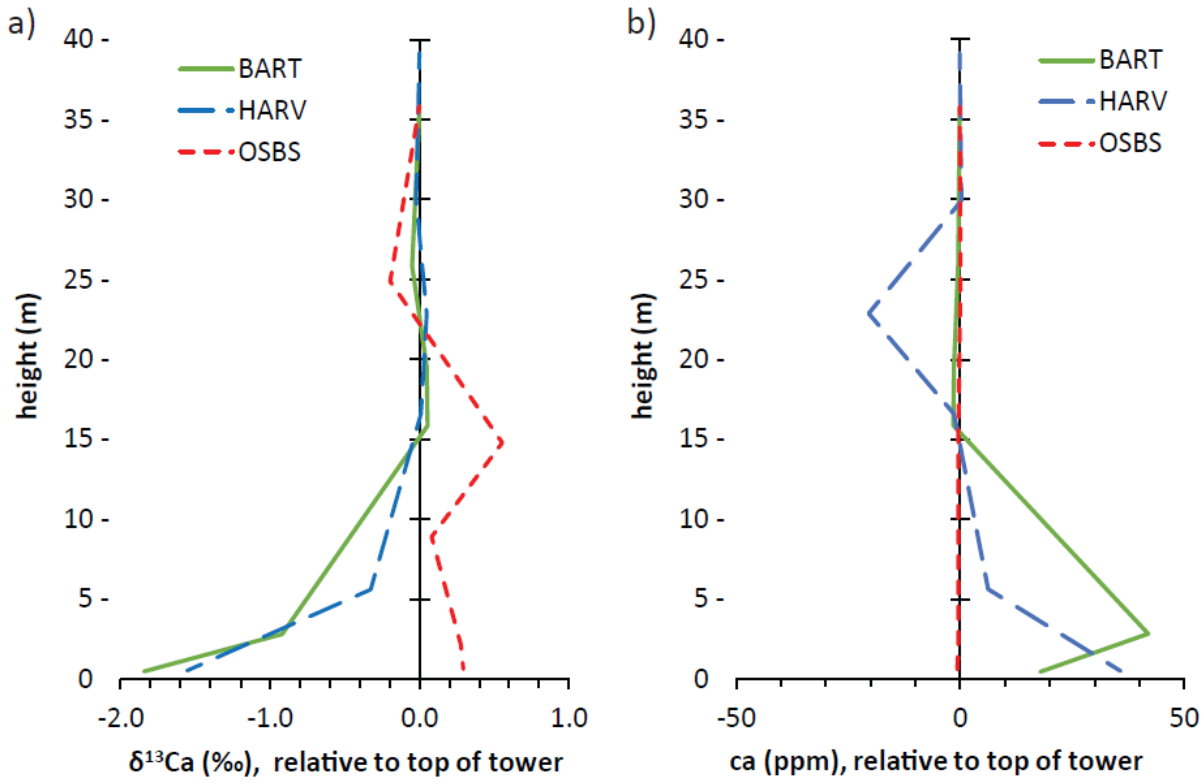

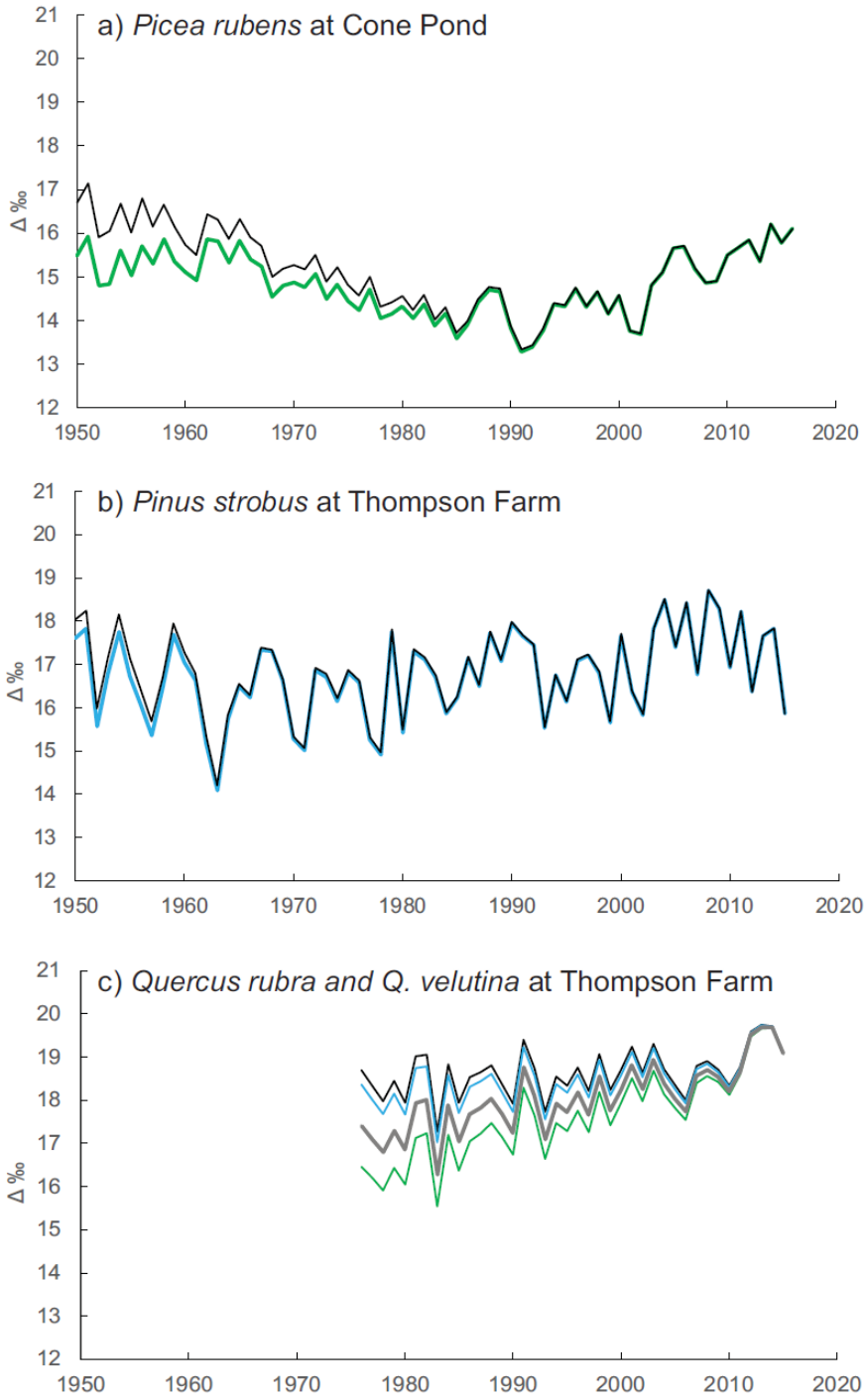

Figure 6: Three example chronologies of ^{13}C discrimination (Δ), shown both uncorrected and corrected for changing tree size. Note that corrections of +1‰ to $\delta^{13}C_p$ translate to approximately a -1‰ change in Δ (see Eq. 2). All else being equal, lower Δ reflects lower c_i/c_a ratios and higher iWUE. Closed-canopy corrections are shown in green, and open-regeneration corrections in blue, as appropriate for each stand. For the *Quercus* chronology, a partial open-canopy correction (gray) is the best approach given what is known about the stand history.

These Δ values are converted to iWUE estimates in Fig S1, using the appropriate c_a and $\delta^{13}C_a$ values for each year.

Supplemental Methods

Sampling for composite isotope chronologies

Samples of *Picea rubens* were collected at the Cone Pond Watershed (Thornton, NH, USA) in October 2016. Sampling points were spaced 30 - 40 m apart along transects that approximately followed contour lines at a range of elevations throughout the watershed. Only apparently healthy trees with a DBH of at least 15 cm were sampled (Table S3); the closest such tree to each sampling point was sampled. Two cores were collected per tree, at approximately breast height. Samples were cross-dated and 8 trees per species, of sufficient age and cross-dating confidence, were selected for annual-resolution composite latewood isotope analysis (1950-2016).

Samples of *Quercus rubra* / *Q. velutina* and *Pinus strobus* were collected in four 900 m^2 plots across two stands 800 m apart at Thompson Farm (Durham, NH, USA) in September 2015 – one stand where we later sampled *Quercus* spp. as described in the main methods above, and another where we later sampled *P. strobus* (Table S2). Species composition, tree age distribution, and disturbance history of the two stands is similar, so samples from the two stands were analyzed together. We sampled all codominant and dominant *Pinus* and *Quercus* in each plot (31 of each species; summary statistics in Table S3). Because some of the trees we sampled were selected for ongoing physiological study, cores were collected at about 30 cm height, and only one core was collected per tree. Samples were cross-dated using standard dendrochronological approaches (Grissino-Mayer 2001, Speer 2010). Seven cores of each species were then selected for isotope analysis, based on tree age and the confidence of cross-dating. To avoid including the earliest ~20 years of growth in our composite samples while keeping the same trees in the sample throughout the chronology, the *Quercus* chronology

extended only back to 1976, and the *P. strobus* chronology to 1950. Latewood was composited for each year and species.

All composite annual samples for each species were extracted to α-cellulose and analyzed for $\delta^{13}C$ as described in the main methods. For both uncorrected and composite isotope chronologies, we calculated iWUE for each year based on Eqs 1-3. For c_a, we used a spline-fit time-series compiled from direct c_a observations starting in 1958, and ice core data prior to 1958 (http://scrippsco2.ucsd.edu/data/atmospheric_co2/icecore_merged_products). For $\delta^{13}C_a$, we used the two-segment linear model (with a breakpoint in 1962) reported by McCarroll and Loader (2004). We validated that the extrapolation of this model continues to parsimoniously describe $\delta^{13}C_a$ at Mauna Loa through the late-2010s.

References

Grissino-Mayer HD (2001) Evaluating crossdating accuracy: A manual and tutorial for the computer program COFECHA. Tree-Ring Res 57:205–221.

McCarroll D, Loader NJ (2004) Stable isotopes in tree rings. Quat Sci Rev 23:771–801.

Speer JH (2010) Fundamentals of Tree-Ring Research. The University of Arizona Press, Tucson, AZ.

Table S1: Explanation of site codes used in Figures 1-3. Additional information on these sites is provided in Table S2.

Site code	Site name	Location	Owner
BJ	Blue Job State Forest	Farmington, NH	NHDFL
CW	College Woods	Durham, NH	UNH
CP	Cone Pond Watershed	Thornton, NH	USFS
EF	East Foss Farm	Durham, NH	UNH
HB	Hubbard Brook Exp. Forest (WS-3 and adjacent)	Woodstock, NH	USFS
J	Jones Property	Milton, NH	UNH
SB	Saddleback Mountain	Deerfield, NH	UNH
SR	Sleepers River Research Watershed (WS-9)	Danville, VT	USGS
TF	Thompson Farm	Durham, NH	UNH

NHDFL = State of New Hampshire, Division of Forests and Lands
UNH = University of New Hampshire
USFS = United States Forest Service
USGS = United States Geological Survey

Table S2: Description of study sites where short tree cores were collected to quantify tree-size effects on $\delta^{13}C_p$. Site codes are explained in Table S1. Soils information was extracted from NRCS soil maps and descriptions (https://websoilsurvey.sc.egov.usda.gov/), or personal observations and landscape interpretation in the field.

Species	Site	Date sampled	S extent	N extent	W extent	E extent	Mean elev (m)	Other major species present	Soil Order	Soil Parent	Soil Drainage
Acer rubrum	**CP**	Mar 2018	43.9055	43.9091	-71.6069	-71.6063	565	PIRU, ABBA, TSCA	Spodosol	till	moderate to excessive
	J	Nov 2017	43.4731	43.4766	-71.0147	-71.0124	150	FAGR, BEAL, ACSA, TSCA	Inceptisol/Entisol	outwash/moraine	somewhat excessive
Acer saccharum	**EF**	Nov 2017	43.1228	43.1232	-70.9396	-70.9392	25	FRAM, ACRU, ROPS, QURU	Inceptisol	glaciolacustrine	moderately well
	J	Nov 2017	43.4731	43.4752	-71.0142	-71.0130	165	FAGR, BEAL, TSCA	Inceptisol	moraine	somewhat excessive
	SR	May 2018	44.4914	44.4944	-72.1632	-72.1599	560	BEAL, FRAM	Inceptisol	till	moderate to well
	HB	May 2018	43.9527	43.9593	-71.7232	-71.7183	560	FRAM, FAGR, BEAL	Spodosol/Inceptisol	till	moderate to well
Fagus grandifolia	**CW**	Nov 2017	43.1142	43.1360	-70.9522	-70.9486	30	PIST, QURU, BELE, PIRE	Inceptisol	till	well to somewhat excessive
	J	Nov 2017	43.4731	43.4759	-71.0146	-71.0124	160	ACSA, BEAL, ACRU	Inceptisol/Entisol	outwash/moraine	somewhat excessive
	HB	May 2018	43.9520	43.9593	-71.7248	-71.7183	560	ACSA, FAGR, BEAL, PIRU	Spodosol/Inceptisol	till	moderate to well
Fraxinus americana	**SR**	May 2018	44.4889	44.4944	-72.1639	-72.1599	560	ACSA, BEAL	Spodosol/Inceptisol	till	moderate to well
	HB	Sep 2018	43.9504	43.9556	-71.7242	-71.7204	510	ACSA, FAGR, BEAL	Spodosol/Inceptisol	till	moderate to well
Picea rubens	**BJ**	Jan 2018	43.3306	43.3331	-71.1169	-71.1168	400	TSCA, PIST, ACRU	Inceptisol	till	well
	CP	Mar 2018	43.9055	43.9093	-71.6069	-71.6063	575	TSCA, ABBA, ACRU	Spodosol	till	well to excessive
	SR	May 2018	44.4963	44.4967	-72.1653	-72.1641	680	ABBA, ACRU	Spodosol	till	poor to well
	HB	May 2018	43.9567	43.9618	-71.7241	-71.7183	680	ACSA, FAGR, BEAL	Spodosol	till	well to excessive
Pinus strobus	**SB**	Feb 2018	43.1713	43.1726	-71.2172	-71.2145	230	QURU, ACRU, TSCA	Inceptisol	till	moderate to excessive
	TF	Nov 2017	43.1126	43.1128	-70.9531	-70.9509	25	QURU, ACRU, TSCA, QUVE	Entisol	outwash	excessive
Quercus rubra	**EF**	Nov 2017	43.1184	43.1217	-70.9369	-70.9328	25	PIST, QUVE, FAGR, ACRU, QUAL	Inceptisol	till	well
	TF	Dec 2017	43.1051	43.1057	-70.9537	-70.9529	25	ACRU, PIST, FAGR, QUVE	Inceptisol	till	well
Tsuga canadensis	**CP**	Mar 2018	43.9055	43.9093	-71.6069	-71.6063	575	PIRU, ACRU, ABBA	Spodosol	till	moderate to well
	J	Nov 2017	43.4750	43.4756	-71.0113	-71.0109	160	ACRU, QURU, PIST	Entisol	outwash/esker	excessive

Additional species codes: ABBA = *Abies balsamea*; BEAL = *Betula alleghaniensis*; ROPS = *Robinia pseudoacacia*; QUAL = *Quercus alba*

Table S3: Description of samples used for the composite $\delta^{13}C$ chronologies to be corrected for changing tree size. Note that all ages are minimum estimates, based on the earliest measured ring in each core.

			Growth chronology								**Isotope chronology**				
Site	Species	Year sampled	n trees cored	n trees Xdated	min diam when sampled	mean diam when sampled	max diam when sampled	min age when sampled	mean age when sampled	max age when sampled	period	n trees	mean age when sampled	mean DBH at start of chron	mean DBH when sampled
CP	PIRU	2016	22	14	17.5	31.2	50.1	59	103	166	1950-2016	8	118	19.9	32.3
TF	PIST	2015	31	31	32.2	52.3	87.6	48	79	109	1950-2015	7	94	26.4	60.4
TF	QURU, QUVE *	2015	31	31	23.6	34.1	44.9	34	46	63	1976-2015	7*	53	13.1	35.0

* all healthy codominant oaks of subgenus *Lobatae* in the sampling plots were sampled together for this analysis, including 15 *Q. rubra*, 15 *Q. velutina*, and 1 *Q. coccinea*. The isotope sample includes three QURU and four QUVE.

Figure S1: Intrinsic WUE from the three example chronologies, shown both uncorrected and corrected for changing tree size. Closed-canopy corrections are shown in green, and open-regeneration corrections in blue, as appropriate for each stand. For the *Quercus* chronology, a partial open-canopy correction (gray) is the best approach given what is known about the stand history.